The Ratio of $W + N$ jets To $Z^0/\gamma^* + N$ jets Versus N As a Precision Test of the Standard Model

Erin Abouzaid and Henry Frisch
Enrico Fermi Institute, University of Chicago
(Dated: May 28, 2003)

We suggest replacing measurements of the individual cross-sections for the production of $W+$ N jets and $Z+$ N jets in searches for new high-energy phenomena at hadron colliders by the precision measurement of the ratios (W+0 jet)/(Z+0 jet), (W+1 jet)/(Z+1 jet), (W+2 jets)/(Z+2 jets),... (W+N jets)/(Z+N jets), with N as large as 6 (the number of jets in $t\bar{t}H$). These ratios can also be formed for the case where one or more of the jets is tagged as a b or c quark. Existing measurements of the individual cross sections for $W \to e\nu+$ N jets at the Tevatron have systematic uncertainties that grow rapidly with N, being dominated by uncertainties in the identification of jets and the jet energy scale. These systematics, and also those associated with the luminosity, parton distribution functions (PDF's), detector acceptance and efficiencies, and systematics of jet finding and b-tagging, are expected to substantially cancel in calculating the ratio of W to Z production in each N-jet channel, allowing a greater sensitivity to new contributions in these channels in Run II at the Tevatron and at the LHC.

PACS numbers: 14.70.Fm, 14.70.Hp, 13.85.-t, 13.85.Rm

INTRODUCTION

The signatures of the leptonic decays of the heavy gauge bosons W or Z^0 accompanied by jets, $W \to \ell\nu+$ jets and $Z^0 \to \ell^+\ell^-+$ jets, are among the preeminent-eminent search channels in very high energy particle collisions for 'new physics', i.e. interactions or particles that are not part of the Standard Model [1–4]. Many extensions of the SM predict new particles which have electroweak (EWK) couplings and decay into the SM gauge bosons W, Z^0 , and γ, accompanied by jets. For example, searches have been made in the W or Z^0 +jets channels for supersymmetric particles [5, 6], technicolored hadrons [7], heavy W' and Z' bosons [8–10] that might arise in extended gauge groups or from excitations in extra spatial dimensions, charged Higgs bosons [11, 12], and leptoquarks [13–16], among others. More generally, any production of new heavy particles with quantum numbers conserved by the strong interaction and EWK couplings is likely to contribute to signatures with one or more EWK gauge bosons; additional jets will always be present at some level from initial-state radiation, and may also be created in cascade decays of new heavy particles or from the decay of associated heavy particles.

Within the SM, the top quark was discovered and its mass measured in the W+3/4 jets channel in which at least one jet was identified as a b-quark [17–20]. The W+ 2 jets channel with b-quark identification has been used to search for the Higgs boson [21] and for single top ($t\bar{b}$) production in the $W+b\bar{b}$ signature [22]. Associated Higgs production via $t\bar{t}H$ is expected to produce W+6 jets, of which 4 are b-quarks; associated W and Z production via $t\bar{t}W$ or $t\bar{t}Z$ will also produce W+6 jets, of which two will be b-quarks.

Precise measurements of the $W + N$ jets [23] and $Z^0/\gamma^* + N$ jets [24] channels, where N is the number of jets, for values of N between 0 and at least 6, including the cases where pairs of the jets are either $b\bar{b}$ or $c\bar{c}$, would thus provide a broad search in a number of possible signatures of physics beyond the SM. The importance of calculating the cross sections for these channels has long been recognized [25–38]; the development of sophisticated Monte Carlo programs capable of handling more particles in the final state at leading order (LO), or in some cases, next-to-leading order (NLO), now enables us to contemplate much more precise tests in the upcoming Tevatron Run II and at the LHC.

However, direct measurements of the production cross sections of $W + N$ jets or $Z^0/\gamma^* + N$ jets signatures suffer from inherent theoretical and experimental uncertainties associated with the definition and measurement (and hence counting) of jets. Among the dominant experimental uncertainties are the energy response of the detector to a jet ('energy scale'), additional energy contributions from the underlying event (that part of the $\bar{p}p$ collision not directly involved in the hard parton-parton collision that produces the W or Z), backgrounds from misidentified non-electroweak events, and jet acceptance. These effects and others can change the number of jets measured in a given event. Uncertainties in the theoretical SM predictions are dominated by the choice of Q^2 scale, the parton distribution function (PDF), initial/final state radiation (ISR/FSR), and the non-perturbative evolution of partons into on-shell particles that would then be detected. All of these effects combined mean that the measurement of a specific exclusive N-jet channel such as W+ 4 jets will be completely dominated by systematic uncertainties at the Tevatron in Run II and at the LHC.

In this note we use the Monte Carlo programs MadGraph [39, 40] and MCFM [41–43] to explore using the measured ratios of $W + N$ jets to $Z^0/\gamma^* + N$ jets at

each value of N to provide a much more precise test of the SM than can be made by measuring the cross sections themselves [44]. The W bosons are assumed to be identified by the leptonic decay $W^+ \to e + \nu$, and the Z^0/γ^* intermediate state by $Z^0/\gamma^* \to e^+e^-$. In most of the above models of new physics the production of new particles decaying into W and Z^0/γ^* + jet final states would change the ratio from its SM prediction. The uncertainties listed above, except the misidentification backgrounds, are expected to cancel to a large degree, and the backgrounds can themselves be made to partially cancel by deriving the $\ell\nu$ and $\ell^+\ell^-$ event samples from a common inclusive high-p_T lepton sample [45]. We use data from the CDF [46] collaboration from Run I at the Fermilab Tevatron to estimate the sensitivity to contributions from non-SM processes using the $\sigma(W + N\text{jets})/\sigma(Z^0/\gamma^* + N\text{jets})$ ratio method.

EXPERIMENTAL UNCERTAINTIES IN $\sigma(W + N\textbf{jets})/\sigma(Z^0/\gamma^* + N\textbf{jets})$

The CDF Collaboration has published comprehensive studies of inclusive [47] $W \to e\nu + N$ jets and $Z^0/\gamma^* \to e^+e^- + N$ jets production in $\bar{p}p$ collisions at $\sqrt{s} = 1.8$ TeV [46]. The DØ collaboration has measured the ratio of cross sections (W+ 1 jet)/(W+0 jet) [48]; as the DØ measurements are less extensive in the number of jets (N) and do not include measurements of Z^0 + jets, we focus here on the CDF measurements.

The CDF W selection required an electron with $E_T >$ 20 GeV and $|\eta| < 1.0$, and missing transverse energy [45] $\not\!\!E_T > 25$ GeV. The Z selection required one electron satisfying the same charged lepton requirements, and a second electron with $E_T > 20$ GeV for $|\eta| < 1.0$, $E_T >$ 15 GeV for $1.1 < |\eta| < 2.4$, and $E_T > 10$ GeV for $2.4 < |\eta| < 3.6$. Jet identification [49] was made with a cone size in η-ϕ space of $\Delta R = 0.4$, a threshold of $E_T > 15$ GeV, and an η range of $|\eta| < 2.5$. Multiple jets were required to be separated from each other in η-ϕ space by a distance $\Delta R > 0.52$; the requirement that the electron be 'isolated' from other clusters of energy in the calorimeter also corresponds to requiring $\Delta R > 0.52$ between the electron and each jet [46].

The individual (exclusive) cross sections extracted from the inclusive cross sections measured by CDF for $W + N$ jets and $Z^0/\gamma^* + N$ jets versus the number of jets, N, are displayed in Table I and Figure 1, after being modified for comparison with MadGraph's W^+predictions by dividing the CDF cross sections for $W^+ + W^-$ by two. The uncertainties have been calculated in two ways: assuming no correlations (giving an upper bound for the uncertainty) and assuming complete correlation (giving a lower bound). The uncorrelated uncertainties at each value of N have been calculated by subtracting the uncertainties of higher values of N in quadrature, and are reported first in the table. This overestimates the uncertainties, but as the (N+1)th channel is typically only 20% of the Nth channel the overestimate is not large. The correlated uncertainties at each value of N have been calculated by subtracting the uncertainties of higher values of N; these uncertainties are reported second in the table.

The estimated CDF systematic uncertainties are broken down according to the source of each uncertainty in Table II versus the inclusive number of jets. One can see that in general the quoted systematic uncertainties grow rapidly with N, as described in detail in Ref. [46] This is due to the difficulties of counting jets given the rapidly falling spectrum in E_T and the uncertainties in measuring the energy of a jet, and, to a lesser extent, uncertainties in the position of the jet with respect to the limit in η in the jet selection. In addition, energy deposited in the calorimeter from the fragments of the collision not directly produced by the 'hard' interaction that produced the boson, called the 'underlying event', contribute to the total energy measured in the jet cone, and can promote jets from below threshold to over threshold, changing the number of jets in the event. Similarly, multiple interactions from separate $\bar{p}p$ collisions in the same bunch crossing [50] can contribute energy in the jet cone. There are smaller contributions from uncertainties in the acceptance for the leptons, for the 'obliteration' of a lepton by a jet (if a jet lands close to a lepton the lepton can fail the identification criteria), and uncertainties in the contribution from decays of the top quark. Lastly, the uncertainty due to backgrounds from processes other than vector boson production ('QCD background') grows with the number of jets.

The largest uncertainty is from the jet energy scale. This uncertainty will cancel in the production of W+jets and Z^0/γ^* + jets events to the extent that the spectra in E_T, the distribution in η, and the composition (e.g. quark versus gluon) of the jets in the two processes are the same [51]. Figure 2 shows the spectra in η and E_T generated with the MadGraph Monte Carlo program [40] at LO. Using the difference of the ratio of the fitted slopes of the E_T distributions for W and Z production in Figure 2 times a typical uncertainty in the E_T scale of 20% [46] at 20 GeV gives an estimate of the uncertainty in the ratio of 2%. The effect of the finite acceptance in η for jets depends on the difference in the distributions in η of jets in W or Z production; taking the difference shown in Figure 2 times the estimated variation with rapidity in jet response [52] gives an estimate of the uncertainty in the ratio of 1%.

The second largest systematic uncertainty is from the effects of energy from the underlying event, which can 'promote' a 3-jet event to being a 4-jet event, for example, by boosting a lower-energy jet above the jet-counting threshold in E_T. We expect that the underlying events in W and in Z events should be very similar; studies of the underlying event in jet events [53] predict that the

TABLE I: The cross sections times branching ratios for $W^+ + N$ jets and $Z^0/\gamma^* + N$ jets production in pb (first two columns) extracted from the CDF measurements versus the number of jets, at $\sqrt{s} = 1.8$ TeV. These are used to calculate the ratios of the $W^+ + N$ jets to $Z^0/\gamma^* + N$ jets jet cross section times branching ratio (third column). Also shown are the (less robust) ratios of $\sigma(W + N\text{jets})/\sigma(W + N + 1\text{jets})$ and $\sigma(Z^0/\gamma^* + N\text{jets})/\sigma(Z^0/\gamma^* + N + 1\text{jets})$. The first uncertainty given is the uncorrelated uncertainty, while the second (in parentheses) is the correlated uncertainty. These uncertainties are derived as discussed in the text.

N	$\sigma_{W^+ + Nj}$ (pb)	σ_{Z+Nj} (pb)	$\sigma_{W^+ + Nj}/\sigma_{Z+Nj}$	$\sigma_{W+Nj}/\sigma_{W+N+1j}$	$\sigma_{Z+Nj}/\sigma_{Z+N+1j}$
0	1010 ± 54 (34)	185.8 ± 11.1 (6.7)	5.43 ± 0.44(0.27)	5.46 ± 0.78(0.53)	5.23 ± 0.87(0.60)
1	185 ± 25 (17)	35.5 ± 5.5 (3.9)	5.21 ± 1.06(0.75)	4.46 ± 1.10(0.81)	4.55 ± 1.26(0.93)
2	41.5 ± 8.7 (6.5)	7.8 ± 1.8 (1.34)	5.32 ± 1.65(1.23)	5.42 ± 1.98(1.30)	4.88 ± 1.97(1.46)
3	7.7 ± 2.3 (1.4)	1.6 ± 0.53(0.39)	4.78 ± 2.14(1.46)	5.28 ± 4.48(3.77)	3.72 ± 1.92(1.73)
4	1.45± 1.15(1.00)	0.43 ± 0.17(0.17)	3.37 ± 2.99(2.68)	-	-

TABLE II: The systematic uncertainties in percent on the measured CDF inclusive $W + N$ jet production cross sections for for N=1 to N=4 (column 1) [46]. The successive columns are the uncertainties in the cross sections due to uncertainties in: the calorimeter jet energy scale, the underlying event, QCD background to W identification, multiple $\bar{p}p$ interactions in a single event, the value of the maximum allowed $|\eta|$ for jets to be counted, the W acceptance, 'obliteration' of an electron by the superposition of a jet, and contributions from the top quark. The larger error bar is quoted in the case of asymmetric uncertainties.

N(Jets)	Et_J Scale	Und Ev	QCD Bkgd	Mult Int	η_J	Acc	Oblit	Top
≥ 1	6.8%	5.8%	5.2%	3.2%	1.9%	0.8%	0.2%	0.05%
≥ 2	11%	9.8%	5.4%	7.2%	3.7%	1.0%	0.3%	0.3%
≥ 3	17%	16%	9.1%	9.8%	4.8%	1.8%	0.6%	1.3%
≥ 4	23%	21%	15.8%	14%	5.5%	3.5%	1.3%	0.5%

contribution from the beam fragments, which could be different due to the different quark diagrams in W and in Z production, are a small portion of the total. However, the energy per tower contributed by the underlying event, and hence the effect on 'promotion' of jets, can be directly measured in $W + N$ jets and $Z^0/\gamma^* + N$ jets events. We consequently assume that this uncertainty will be negligible in the ratio.

For higher (≥ 4) jet multiplicities QCD backgrounds become comparable to each of the above. The backgrounds in the Z^0/γ^* channel are at the few percent level, and are measurable (and hence subtractable) by counting same-sign events. Previous studies of the backgrounds to inclusive W production by CDF [54] for selection criteria similar to those used here have shown that the background is dominated by approximately equal contributions from leptons from heavy flavor production and misidentified hadrons. How well these can be measured with the new Run II detectors is not yet known; the former can be measured with the silicon vertex detectors, and the latter can be measured by conventional background techniques.

The next largest systematic uncertainty in the Run I CDF cross section, contributions from multiple $\bar{p}p$ interactions, should cancel identically in the ratio, as it is uncorrelated with the hard scattering.

The remaining uncertainties due to acceptance, 'obliteration' of a lepton by a jet, and contributions from top decay, are at most at the few percent level [46].

MONTE CARLO PROGRAMS AND EVENT SELECTION CRITERIA

We have explored the $W^+$to Z^0 ratios in $\bar{p}p$ collisions at the Tevatron energy of $\sqrt{s} = 1.96$ TeV using the Monte Carlo programs MadGraph [40] and MCFM [43]. Samples of $W^+(\rightarrow e^+\nu) + N$ jets and $Z^0/\gamma^* (\rightarrow e^+e^-) + N$ jets , for N up to 4, were produced at LO using MadGraph. MCFM was used to explore the ratios for up to 2 jets at NLO, and to understand the dependence of the ratios on the Q^2 scale and on the parton distribution functions for up to 4 jets at LO. Jets are treated at the 'parton level' with kinematic selections applied to the 4-vectors with no fragmentation or detector simulation.

We consider only the production in first-order electroweak processes of the W+jets and Z+jets channels – i.e. production of boson + jets from the WW, WZ, and ZZ channels are excluded. We also exclude $t\bar{t}$ and $t\bar{b}$ production; the method proposed here should allow a more precise determination of the non-top W+jets production, the dominant background in the top channel, and hence should allow more precise measurements of the top quark mass and cross section.

The selection criteria and strategy for $W^+$and Z^0/γ^* events used in the Monte Carlo studies were previously developed for the measurement of R, the ratio of cross sections $R \equiv \sigma(W)/\sigma(Z^0/\gamma^*)$ [55]. To minimize systematic uncertainties in the ratio due to the trigger and lepton selection, both W and Z^0/γ^* events are selected from a common sample of inclusive central high transverse momentum [45] (p_T) leptons, with transverse

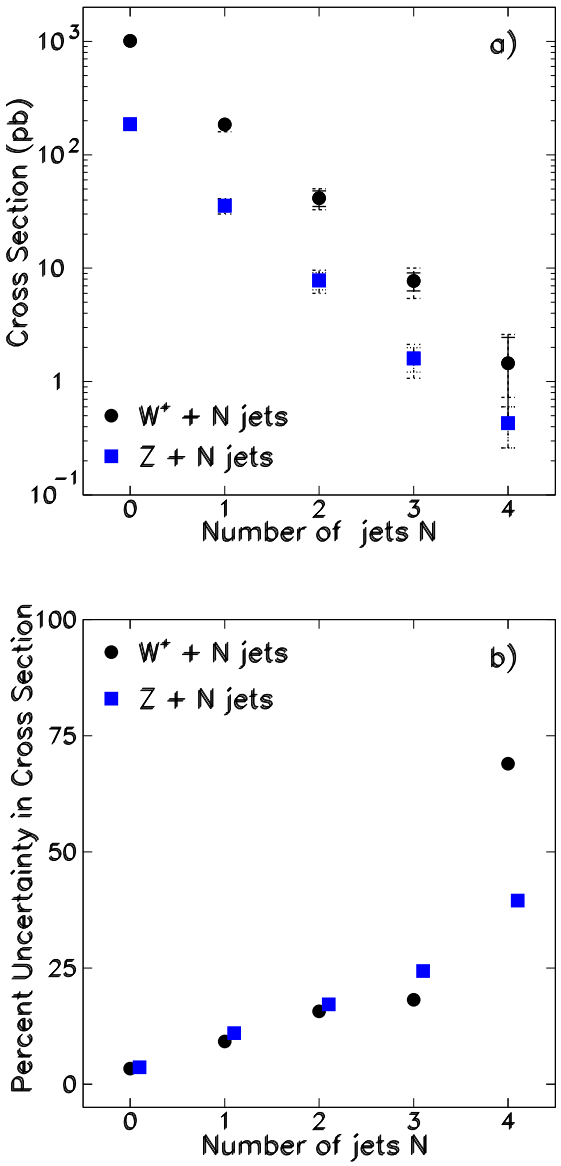

FIG. 1: a) The measured cross sections for the signatures $W^+(\rightarrow e^+\nu)$ + N jets and Z^0/γ^* $(\rightarrow e^+e^-)$ + N jets versus the number of jets, N, in W^+ and Z^0/γ^* production in $\bar{p}p$ collisions at $\sqrt{s} = 1.8$ TeV. The data are from the CDF [46] collaboration and were originally reported as inclusive cross sections. In computing exclusive cross sections from these, the uncertainties have been calculated in two ways. The dotted error bars were calculated assuming no correlations (giving an upper bound for the uncertainty) and the solid error bars were calculated assuming complete correlation (giving a lower bound); b) the percent uncertainty in the $W^+ + N$ jets and Z^0/γ^* + N jets cross sections. The uncertainties shown are the lower bounds (corresponding to the solid error bars in plot a). The figure shows the rapid growth of the uncertainties with N, the number of jets.

energy (E_T) greater than 25 GeV and pseudo-rapidity ($|\eta|$) less than 1.0. The second lepton from the boson decay, either another charged lepton (from Z^0/γ^* decay) or a neutrino (from W decay), is required to have $E_T > 25$ GeV; in the neutrino case this is implemented by requiring the missing transverse energy ($\not\!\!E_T$) to be greater than 25 GeV.

Jets are required to have $E_T > 15$ GeV and to be within $|\eta| < 2.5$. Our MC studies are at parton level, so that there are no considerations of cone size, energy scale, or acceptance corrections in the Monte Carlo numbers.

THE PREDICTED RATIOS $\sigma(W^+ + N\mathbf{jets})/\sigma(Z^0/\gamma^* + N\mathbf{jets})$

The MadGraph predicted LO ratios $\sigma(W^+ + N\text{jets})/\sigma(Z^0/\gamma^* + N\text{jets})$ are presented in Figure 3 and in Table III. To determine the final uncertainty on this ratio will take a full analysis of the Run II data set; in lieu of this we have made some simple assumptions to get an estimate of the sensitivity in cross-section for non-SM physics in each of the N-jet channels in Run II of the Tevatron. We assume that the jet energy response of the calorimeter will largely cancel for jets in Z^0/γ^* events and W events as discussed below. We also assume the effects of the underlying event in Z^0/γ^* and W events will similarly cancel. These are the two largest contributors to the systematic uncertainties quoted in Ref. [46].

THE PREDICTED RATIOS $\sigma(W + N\mathbf{jets})/\sigma(W + N + 1\mathbf{jets})$ AND $\sigma(Z^0/\gamma^* + N\mathbf{jets})/\sigma(Z^0/\gamma^* + N + 1\mathbf{jets})$

While the ratios of cross sections $\sigma(W + N\text{jets})/\sigma(W + N + 1\text{jets})$ and $\sigma(Z^0/\gamma^* + N\text{jets})/\sigma(Z^0/\gamma^* + N + 1\text{jets})$ are much more difficult to measure precisely than the $\sigma(W^+ + N\text{jets})/\sigma(Z^0/\gamma^* + N\text{jets})$ ratios, we include the MadGraph generator-level LO predictions for them here as they are often used in extrapolations in N to estimate backgrounds at large N, and also to measure the strong interaction coupling. These are reported in Table III, and shown in Figure 4.

THE PREDICTED RATIOS AT NEXT-TO-LEADING ORDER

MCFM is capable of calculating cross sections for bosons plus up to 2 jets at next-to-leading order. These predictions and the corresponding results for the ratios $\sigma(W^+ + N\text{jets})/\sigma(Z^0/\gamma^* + N\text{jets})$, $\sigma(W + N\text{jets})/\sigma(W + N + 1\text{jets})$ and $\sigma(Z^0/\gamma^* + N\text{jets})/\sigma(Z^0/\gamma^* + N + 1\text{jets})$ are shown in Table IV. To allow comparison of these MCFM next-to-leading order results to the MadGraph leading order results, the ratios $\sigma(W^+ +$

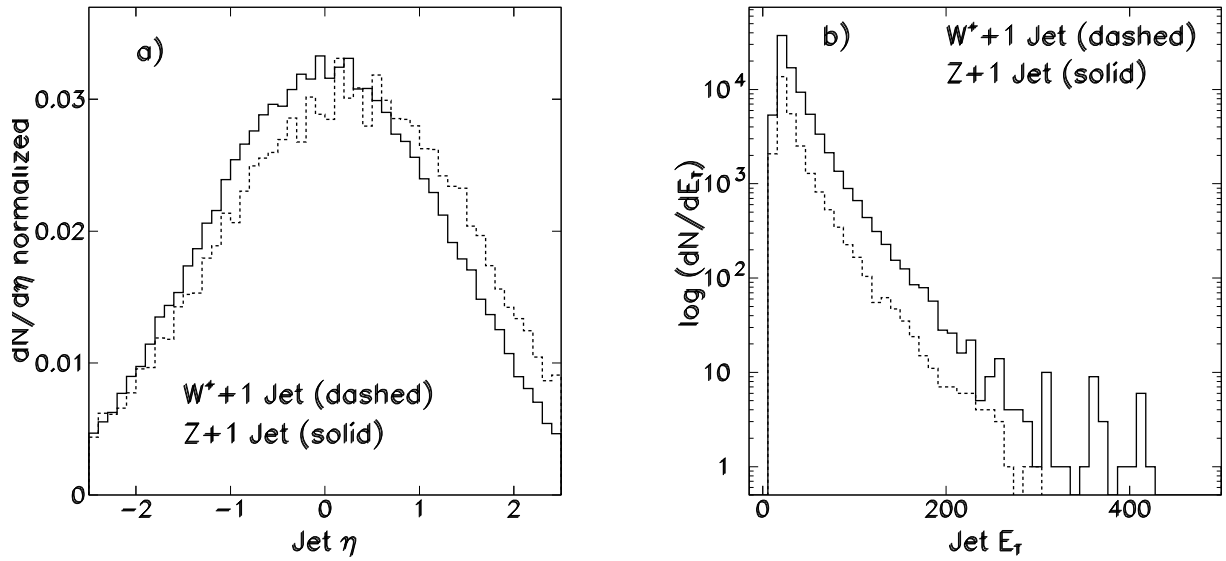

FIG. 2: The plot on the left (a) shows the (normalized) jet η distributions for $W^+(\rightarrow e^+\nu)$ + 1 jet (dashed) and Z^0/γ^* $(\rightarrow e^+e^-)$ + 1 jet (solid) events satisfying the selection criteria described in the text. The plot on the right (b) shows the corresponding jet E_T distributions, log (dN/dE_T) versus N. Both plots are predictions at LO using MadGraph [40]. Uncertainties in the ratios $\sigma(W^+ + N\text{jets})/\sigma(Z^0/\gamma^* + N\text{jets})$ due to the uncertainty in the jet rapidity cut at η=2.5 are estimated from the shapes in the left-hand plot, and those due to the uncertainty in the jet energy scale from the right-hand plot.

TABLE III: MadGraph leading order predictions of cross sections times branching ratio for $W^+ + N$ jets and $Z^0/\gamma^* + N$ jets production in pb (first two columns) versus the number of jets, at $\sqrt{s} = 1.96$ TeV, which are used to calculate the ratios of the $W^+ + N$ jets to $Z^0/\gamma^* + N$ jets jet cross section times branching ratio (third column). Also shown are the (less robust) ratios of $\sigma(W + N\text{jets})/\sigma(W + N + 1\text{jets})$ and $\sigma(Z^0/\gamma^* + N\text{jets})/\sigma(Z^0/\gamma^* + N + 1\text{jets})$ (last two columns).

N	$\sigma_{W^+ + Nj}$ (pb)	σ_{Z+Nj} (pb)	$\sigma_{W^+ + Nj}/\sigma_{Z+Nj}$	$\sigma_{W+Nj}/\sigma_{W+N+1j}$	$\sigma_{Z+Nj}/\sigma_{Z+N+1j}$
0	341.5 ± 0.5	67.0 ± 0.2	5.10 ± 0.02	8.11 ± 0.06	6.41 ± 0.02
1	42.1 ± 0.3	10.45 ± 0.01	4.03 ± 0.03	5.08 ± 0.05	4.91 ± 0.07
2	8.28 ± 0.05	2.13 ± 0.03	3.89 ± 0.06	4.93 ± 0.07	4.75 ± 0.09
3	1.68 ± 0.02	0.448 ± 0.006	3.75 ± 0.07	4.71 ± 0.09	5.15 ± 0.09
4	0.357 ± 0.005	0.087 ± 0.001	4.10 ± 0.07	-	-

$N\text{jets})/\sigma(Z^0/\gamma^* + N\text{jets})$ are plotted in Figure 3, and the ratios $\sigma(W + N\text{jets})/\sigma(W + N + 1\text{jets})$ and $\sigma(Z^0/\gamma^* + N\text{jets})/\sigma(Z^0/\gamma^* + N + 1\text{jets})$ are plotted in Figure 4. The NLO predictions are close to the LO predictions for the ratios $\sigma(W^+ + N\text{jets})/\sigma(Z^0/\gamma^* + N\text{jets})$ and have a similar shape to the LO predictions for the ratios $\sigma(W + N\text{jets})/\sigma(W + N + 1\text{jets})$ and $\sigma(Z^0/\gamma^* + N\text{jets})/\sigma(Z^0/\gamma^* + N + 1\text{jets})$.

THEORETICAL UNCERTAINTIES IN $\sigma(W^+ + N\text{jets})/\sigma(Z^0/\gamma^* + N\text{jets})$

The two largest uncertainties in the predicted LO $W + N$ jets and $Z^0/\gamma^* + N$ jets cross sections are expected to be due to choice of Q^2 scale and parton distribution function (PDF). We investigate the dependence of the ratio on these two choices using MCFM.

Dependence on the Q^2 Scale

The effect of the choice of Q^2 scale is expected to partially cancel in $W + N$ jets and $Z^0/\gamma^* + N$ jets production, as both proceed through a Drell-Yan-like process. We define $W_N^+(Q^2) \equiv \sigma W^+ + N$ jets evaluated at Q^2, and, similarly, $Z_N(Q^2) \equiv \sigma Z^0/\gamma^* + N$ jets . The ratios of W and Z cross sections evaluated at $\mathrm{Q^2 = M_V{}^2}$ and at $\mathrm{Q^2 = M_V{}^2 + P_{T,V}{}^2}$, $W_N^+(M^2)$ $/W_N^+(P_t^2 + M^2)$ and $Z_N(M^2)$ $/Z_N(P_t^2 + M^2)$, are given in Table V and shown in Figure 5. Changing the Q^2 scale affects the W cross sections by as much as 15% and affects the Z cross sections by as much as 12%. However, changing the Q^2 scale has much less effect on the predicted ratio $\sigma(W^+ + N\text{jets})/\sigma(Z^0/\gamma^* + N\text{jets})$, which changes less than 2%, as shown in Figure 6 and in Table V, where the W/Z ratios evaluated at the two different values of

TABLE IV: MCFM next-to-leading order predictions of cross sections times branching ratio for $W^+ + N$ jets and $Z^0/\gamma^* + N$ jets production in pb (first two columns) versus the number of jets, at $\sqrt{s} = 1.96$ TeV, which are used to calculate the ratios of the $W^+ + N$ jets to $Z^0/\gamma^* + N$ jets jet cross section times branching ratio (third column). Also shown are the (less robust) ratios of $\sigma(W + N\text{jets})/\sigma(W + N + 1\text{jets})$ and $\sigma(Z^0/\gamma^* + N\text{jets})/\sigma(Z^0/\gamma^* + N + 1\text{jets})$ (last two columns).

N	$\sigma_{W^+ + Nj}$ (pb)	σ_{Z+Nj} (pb)	$\sigma_{W^+ + Nj}/\sigma_{Z+Nj}$	$\sigma_{W+Nj}/\sigma_{W+N+1j}$	$\sigma_{Z+Nj}/\sigma_{Z+N+1j}$
0	388 ± 1	77.4 ± 0.3	5.01 ± 0.02	6.97 ± 0.04	5.93 ± 0.04
1	55.7 ± 0.3	13.06 ± 0.07	4.27 ± 0.03	4.04 ± 0.04	3.79 ± 0.06
2	13.8 ± 0.1	3.45 ± 0.05	4.00 ± 0.06	-	-

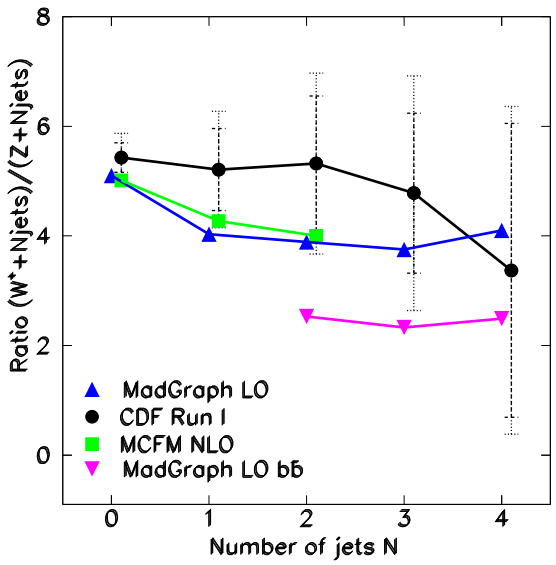

FIG. 3: A comparison of CDF data (circles) with MadGraph leading order predictions (triangles) and MCFM next-to-leading order predictions (squares) for the ratio of production cross sections times leptonic branching ratios for the signature $W^+ + N$ jets to the signature $Z^0/\gamma^* + N$ jets , $\sigma(W^+ + N\text{jets})/\sigma(Z^0/\gamma^* + N\text{jets})$, versus the number of jets, N, in W^+ and Z^0/γ^* production at $\sqrt{s} = 1.8$ TeV for the data and at $\sqrt{s} = 1.96$ TeV for the predictions. The case where two of the jets are b-quark jets are also shown (inverted triangles). The statistical uncertainties on the predictions are smaller than the symbols.

Q^2 also are listed.

Dependence on the Choice of Parton Distribution Function

We have used the MCFM generator and a selection of parton distribution functions to investigate the dependence of the cross sections in the W^++2jets and Z^0 +2jets channels. The cross sections calculated with the CTEQ3L, CTEQ4L [56], MRST98 [57], and MRSG95 [58] distributions were compared to the results calculated with CTEQ5L, the default PDF. The results of the comparison are reported in Table VI. Figure 7 gives the ratio of $\sigma(W^+$+2jets for PDF x) to $\sigma(W^+$+2 jets for CTEQ5L), while Figure 8 shows the ratio of $\sigma(W^+$+2 jets) to σ(Z+2 jets) for a given PDF. For the four PDF's we chose, the changes in the W and Z cross sections themselves range from +27% to -7% for the W's and +25% to -8% for the Z's, while the the range of the change in the ratio is from +1.5% to zero, a factor of ~ 20 smaller [59].

SENSITIVITY TO NEW CONTRIBUTIONS TO THE $\sigma(W + N\text{jets})/\sigma(Z^0/\gamma^* + N\text{jets})$ RATIO

A non-Standard Model source of W+ jets or Z + jets would result in a measured deviation from the expected SM value of the $R_N = \sigma(W + N\text{jets})/\sigma(Z^0/\gamma^* + N\text{jets})$. Assuming that the contribution is to W+jets, we can (crudely) estimate the sensitivity to new physics in each of the $W+$ N-jet channels by multiplying the uncertainty on the ratio $\sigma(W + N\text{jets})/\sigma(Z^0/\gamma^* + N\text{jets})$ by the exclusive $W + N$ jets cross section (if instead the source feeds Z+ jets at the same crossection, the sensitivity will be larger by a factor of about 10 [60].

The estimates above of the systematic uncertainties on R_N are on the order of several percent; an estimate based on the Run I CDF experience in measuring R is that 1% in that ratio may be achievable [54]. Statistical uncertainties would then be expected to dominate over systematics in Run II at the Tevatron for N greater than 2.

Making the assumptions that the new contributions are to the W cross section and not that of the Z, that the systematics on the ratio can be reduced with a much larger dataset [61] from several percent to 1%, and that one uses only the electron modes of W and Z decays, we find the 1-sigma cross-section uncertainties on new physics shown in Table VII. The muon channel would be expected to double the statistics (and hence lower the uncertainties by $\sqrt{2}$).

Additional sensitivity can come from comparing observed with expected kinematic distributions or by looking for additional objects in the events. In particular, the production of a pair of b-quarks suppresses the cross section over that for light quark production by a large factor, in principle allowing a corresponding increase in sensitivity. Table VIII shows the ratio of the QCD cross section for producing N jets including no b quarks to N jets including two b quarks, for W or Z production. How-

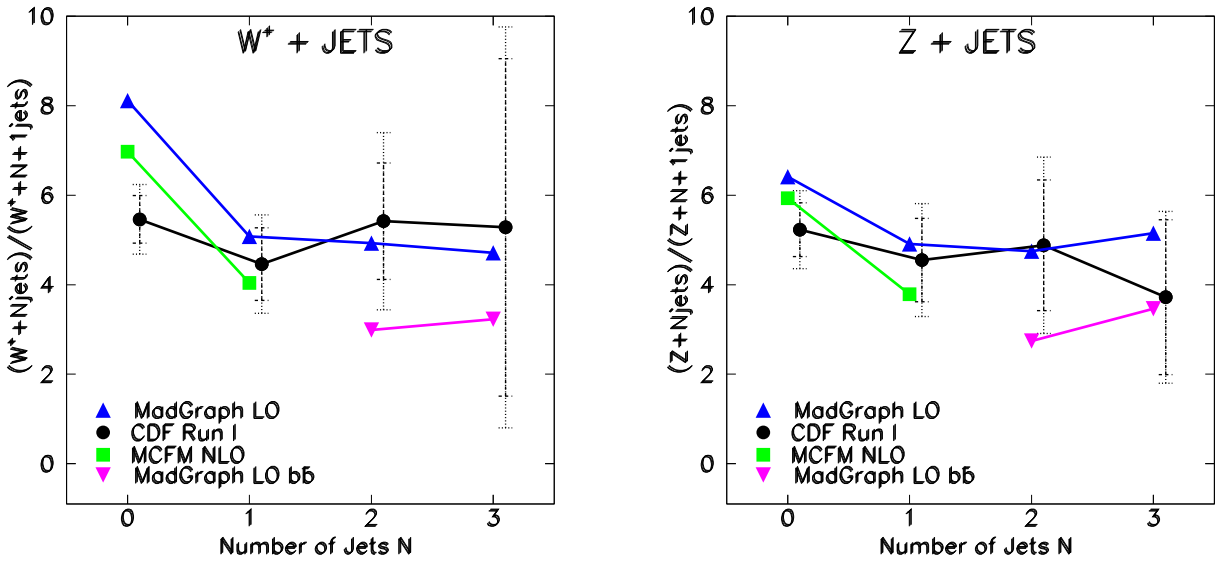

FIG. 4: The ratio of cross sections times branching ratios, $\sigma(W^+ + N\text{jets})/\sigma(W^+ + N + 1\text{jets})$ (left hand plot) and $\sigma(Z^0/\gamma^* + N\text{jets})/\sigma(Z^0/\gamma^* + N + 1\text{jets})$ (right hand plot) versus the number of jets, N, in W and Z production at $\sqrt{s} = 1.8$ TeV for the data and at $\sqrt{s} = 1.96$ TeV for the predictions. The data (circles) are from the CDF [46] and DØ [48] collaborations; the predictions are at leading order from MadGraph [40] (triangles) and next-to-leading order from MCFM [43] (squares). The MadGraph cross sections for when the jets are from gluons or light quarks are shown with triangles, while inverted triangles represent when two of the jets are from b-quarks. Note that the statistical uncertainties on the predictions are smaller than the symbols.

TABLE V: MCFM predictions for the ratios $W^+ + N$ jets and $Z^0/\gamma^* + N$ jets with different Q^2 scales (columns one and two), and the ratio R^+ with different Q^2 scales. R^+ is $\sigma(W^+ + N\text{jets})/\sigma(Z^0/\gamma^* + N\text{jets})$, and $Q_1{}^2$corresponds to $Q^2 = M_V{}^2$, while $Q_2{}^2$corresponds to $Q^2 = M_V{}^2 + P_{T,V}{}^2$.

N_{jets}	$\sigma W^+(Q_1{}^2)$ / $\sigma W^+(Q_2{}^2)$	σZ^0 $(Q_1{}^2)$ / σZ^0 $(Q_2{}^2)$	$R^+(Q_1{}^2)$ / $R^+(Q_2{}^2)$
0	0.999 ± .001	1.000 ± .001	0.999 ± .001
1	1.017 ± .003	1.018 ± .002	0.999 ± .002
2	1.075 ± .002	1.066 ± .002	1.009 ± .002
3	1.153 ± .004	1.134 ± .002	1.017 ± .004

ever standard model top production will provide a large background for non-standard model physics in these signatures.

CONCLUSIONS

The measurement of the production cross sections of the vector bosons $W^\pm$ and Z^0 in association with a number (N) of jets is now a standard way of looking for the production of new particles or processes that are not described by the Standard Model. With the expected increased luminosities of Run II and the LHC, N can be quite large; processes such as associated production of a Higgs boson with a $t\bar{t}$ pair can produce W+ 6 jets (4 of which are b-quarks), for instance. Increasing the precision of the comparison with Standard Model predictions is necessary, as there are truly difficult problems, both theoretical and experimental, in predicting the cross sections for $W + N$ jets and $Z^0/\gamma^* + N$ jets when N is large.

Using the Monte Carlo generators MadGraph and MCFM at the parton level, and the published CDF data on W and Z + jets production, we have made initial estimates of the systematic limits on the precision that can be achieved in the measurement of the ratios of W to Z production, $\sigma(W + N\text{jets})/\sigma(Z^0/\gamma^* + N\text{jets})$, as a function of the number of observed jets, N. The results indicate that the ratios are at least an order-of-magnitude less sensitive to experimental and statistical uncertainties than the individual cross sections. In particular the ratios are more robust for large values of N, where the experimental uncertainties in the energy scale and contributions from the underlying event and multiple interactions lead to a rapid growth in the cross section uncertainty with N.

TABLE VI: MCFM predictions for the ratios W^++2jets and Z^0 +2jets with different PDF's. The PDF's that were compared are CTEQ3L, CTEQ4L, CTEQ5L, MRSG95, MRST98. Column one gives the ratio of $\sigma(W^+$+2jet) at one of the PDF's to $\sigma(W^+$+2jets) at CTEQ5L. Column two is the analogous Z^0 information. The third column is the ratio of $R^+(2)$ at a specific PDF to $R^+(2)$ at CTEQ5L, where $R^+(2)= \sigma(W^+ + 2\text{jets})/\sigma(Z^0/\gamma^* + 2\text{jets})$.

PDF X	$(\sigma \mathrm{W}^+_\mathrm{X})$ / $(\sigma \mathrm{W}^+_\mathrm{L})$	$(\sigma \mathrm{Z}_\mathrm{X})$ / $(\sigma \mathrm{Z}_\mathrm{L})$	$(\mathrm{R}^+_\mathrm{X})$ / $(\mathrm{R}^+_\mathrm{L})$
CTEQ5L	1.000 ± .000	1.000 ± .000	1.000 ± .000
CTEQ3L	1.103 ± .002	1.090 ± .002	1.011 ± .003
CTEQ4L	1.105 ± .002	1.094 ± .002	1.009 ± .003
MRSG95	1.268 ± .002	1.249 ± .002	1.015 ± .003
MRST98	0.932 ± .001	0.922 ± .001	1.011 ± .002

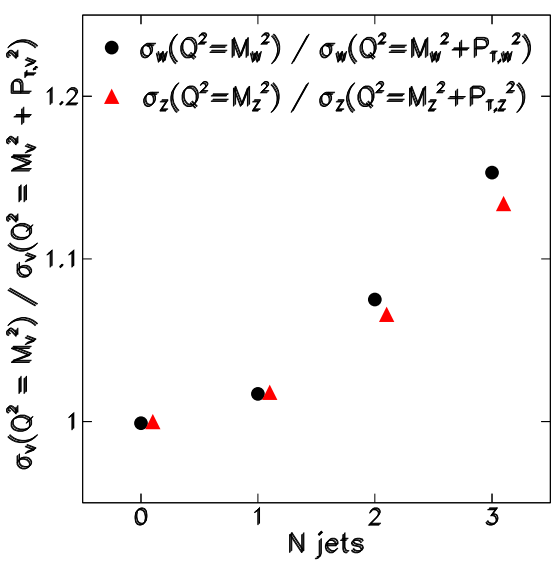

FIG. 5: The ratios $\sigma(W^+ + N$ jets at $\mathrm{Q}^2 = \mathrm{M_V}^2)$ to $\sigma(W^+ + N$ jets at $\mathrm{Q}^2 = \mathrm{M_V}^2 + \mathrm{P_{T,V}}^2)$ and $\sigma(Z^0/\gamma^* + N$ jets at $\mathrm{Q}^2 = \mathrm{M_V}^2)$ to $\sigma(Z^0/\gamma^* + N$ jets at $\mathrm{Q}^2 = \mathrm{M_V}^2 + \mathrm{P_{T,V}}^2)$. Changing the Q^2 scale significantly changes the cross sections, by up to approximately 15%. However the ratio of W to Z cross sections changes much less (see Table V).

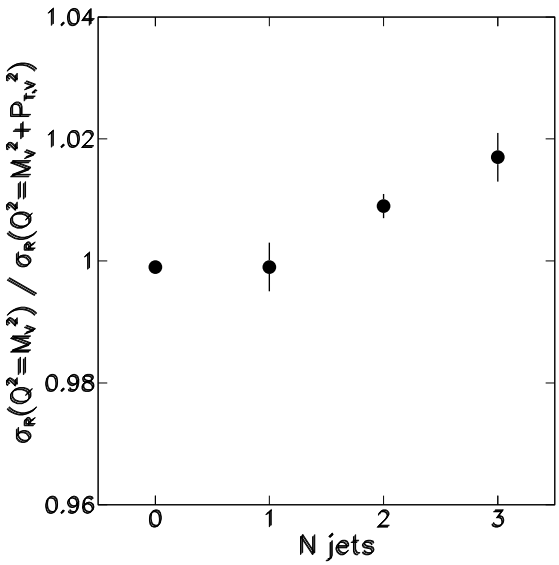

FIG. 6: The ratios (R^+ at $\mathrm{Q}^2 = \mathrm{M_V}^2$) to ($R^+$ at $\mathrm{Q}^2 = \mathrm{M_V}^2 + \mathrm{P_{T,V}}^2$), where $R^+ = \sigma(W^+ + N\text{jets})/\sigma(Z^0/\gamma^* + N\text{jets})$. Changing the Q^2 scale affects this ratio by $\sim 2\%$ while the individual cross sections change by more than 15%.

With respect to the theoretical uncertainties, at N=2, for example, we find the uncertainty due to choice of Q^2 scale is a factor of ~ 8 smaller in the ratio $\sigma(W + N\text{jets})/\sigma(Z^0/\gamma^* + N\text{jets})$ than in the individual W or Z cross sections. Similarly, the uncertainty due to the choice of PDF, largely driven by the u/d quark ratio, is smaller in the ratio by a factor of $\sim$20.

The experimental uncertainties in the cross sections, dominated by the uncertainty in the jet energy scale and contributions from the underlying event, are greatly diminished by focusing on the ratio of W and Z^0/γ^* cross sections ratio than the cross sections themselves. In particular the uncertainty due to uncertainties in the jet energy scale, the contributions from the underlying event, multiple interactions in one event, etc. cancel to a high degree. We have here made estimates at the parton level; a full determination of these will require the new data and a full analysis; our initial estimates are that the ratios can be determined at the several percent level. This is a significant improvement over the present uncertainties on the cross sections themselves.

It is a pleasure to acknowledge helpful conversations with Edward Boos, John Campbell, Jay Dittman, Lev Dudko, Keith Ellis, Michelangelo Mangano, Stephen Mrenna, Jon Rosner, and Tim Stelzer. Special thanks are due to Tim Stelzer and John Campbell for help with MadGraph and MCFM, respectively. This work was supported by the National Science Foundation, grant PHY02-01792.

[1] S. L. Glashow, Nucl. Phys. **22** (1961).
[2] S. Weinberg, Phys. Rev. Lett. **19** (1967).
[3] A. Salam, Proc. 8th Nobel Symposium, Stockholm

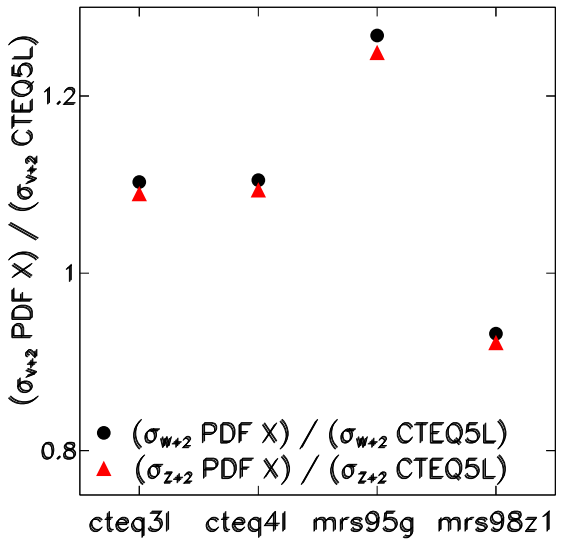

FIG. 7: The ratios σ(W+2jets for PDF X) to σ(W+2jets for CTEQ5L) and σ(Z+2jets for PDF X) to σ(Z+2jets for CTEQ5L). Changing the PDF affects the cross sections quite significantly, by up to approximately 25%. However the ratio of W to Z cross sections changes much less (see Table VI).

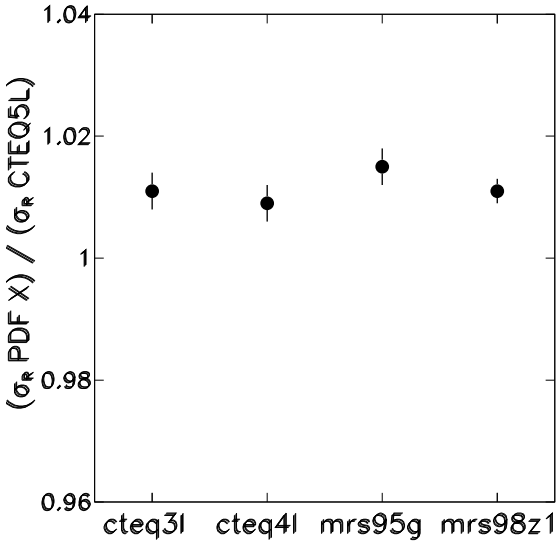

FIG. 8: The ratios R for PDF X to R for CTEQ5L, where R = $\sigma(W + N\text{jets})/\sigma(Z^0/\gamma^* + N\text{jets})$. Changing the PDF affects this ratio much less - by at most 2% - than it affects the individual cross sections.

TABLE VII: The cross section corresponding to a 1-sigma uncertainty in the W/Z ratio in 2 fb^{-1}, and in 15 fb^{-1}. The bins up through N=4 use the cross sections of [46]; the N=5 and higher bins have been extrapolated using an exponential, with a factor of 4.8 for each successive jet. Note that the number of $Z^0 \rightarrow e^+e^-$ events in each bin will be approximately a factor of 10 smaller than the corresponding number of W events. Using the dimuon channel one can gain a factor of approximately $\sqrt{2}$ on these uncertainties.

Event and W Properties		W/Z Ratio Method Reach	
N(Jets)	σ_W	σ_{new} 2 fb^{-1}	σ_{new} 15 fb^{-1}
0	1896 pb	20 pb (1.0%)	20 pb (1.0%)
1	370 pb	4.4 pb (1.2%)	3.7 pb (1.0%)
2	83 pb	1.5 pb (1.8%)	0.9 pb (1.1%)
3	15 pb	0.5 pb (3.5%)	240 fb (1.6%)
4	3.1 pb	230 fb (7.5%)	95 fb (2.9%)
5	650 fb	100 fb (16%)	40 fb (6%)
6	140 fb	50 fb (36%)	18 fb (13%)
7	28 fb	20 fb (78%)	8 fb (29%)
8	6 fb	——	4 fb (63%)

(1979).
[4] S. Berman, J. Bjorken, and J. Kogut, Phys. Rev. D **4** (1971).
[5] T. Affolder et al. (CDF), Phys. Rev. **D63**, 091101 (2001), hep-ex/0011004.
[6] D. Acosta et al. (CDF), Phys. Rev. **D65**, 052007 (2002), hep-ex/0109012.
[7] T. Affolder et al. (CDF), Phys. Rev. Lett. **84**, 1110 (2000).
[8] S. Abachi et al. (D0), Phys. Rev. Lett. **76**, 3271 (1996), hep-ex/9512007.
[9] T. Affolder et al. (CDF), Phys. Rev. Lett. **88**, 071806 (2002), hep-ex/0108004.
[10] D. Acosta et al. (CDF) (2002), hep-ex/0209030.
[11] B. Abbott et al. (D0), Phys. Rev. Lett. **82**, 4975 (1999), hep-ex/9902028.
[12] T. Affolder et al. (CDF), Phys. Rev. **D62**, 012004 (2000), hep-ex/9912013.
[13] B. Abbott et al. (D0), Phys. Rev. Lett. **80**, 2051 (1998), hep-ex/9710032.
[14] F. Abe et al. (CDF), Phys. Rev. Lett. **79**, 4327 (1997), hep-ex/9708017.
[15] B. Abbott et al. (D0), Phys. Rev. Lett. **84**, 2088 (2000), hep-ex/9910040.
[16] T. Affolder et al. (CDF), Phys. Rev. Lett. **85**, 2056 (2000), hep-ex/0004003.
[17] F. Abe et al. (CDF), Phys. Rev. Lett. **73**, 225 (1994), hep-ex/9405005.
[18] F. Abe et al. (CDF), Phys. Rev. **D50**, 2966 (1994).
[19] F. Abe et al. (CDF), Phys. Rev. Lett. **74**, 2626 (1995), hep-ex/9503002.
[20] S. Abachi et al. (D0), Phys. Rev. Lett. **74**, 2632 (1995), hep-ex/9503003.
[21] F. Abe et al. (CDF), Phys. Rev. Lett. **81**, 5748 (1998).
[22] D. Acosta et al. (CDF), Phys. Rev. D **65**, 091102 (2002), hep-ex/0110067.
[23] Because the Monte Carlo programs specifically ask for the sign of the final state charged lepton, we use the production crossection for only one sign (W^+) of W production, resulting in ratios R^+ which are half (~ 5) of the usually quoted $R = (W^+ + W^-)/Z^0/\gamma^*$ (~ 10).
[24] The production in the charged dilepton channels (e.g. e^+e^-) proceed through two s-channel amplitudes, the γ and Z^0 poles. While the Z^0 pole dominates for the selection criteria used here ($\sim$ 96%), both amplitudes must always be included (experimentalists have evolved

(N jets) / ($b\bar{b}$+(N-2) jets) for W^+or Z^0/γ^*		$W^+ + b\bar{b} + N$ jets $/Z^0/\gamma^* + b\bar{b} + N$ jets	
W^++2j/$W^+b\bar{b}$+0j: 90.29 ± .96	Z+2j/Z$b\bar{b}$+0j: 58.84 ± .89	$W^+b\bar{b}$+0j/Z$b\bar{b}$+0j:	1.53 ± .03
W^++3j/$W^+b\bar{b}$+1j: 54.72 ± .84	Z+3j/Z$b\bar{b}$+1j: 33.94 ± .69	$W^+b\bar{b}$+1j/Z$b\bar{b}$+1j:	1.61 ± .04
W^++4j/$W^+b\bar{b}$+2j:37.58 ± 1.30	Z+4j/Z$b\bar{b}$+2j: 22.83 ± .40	$W^+b\bar{b}$+2j/Z$b\bar{b}$+2j:	1.65 ± .06

TABLE VIII: Ratios of the cross sections for $W^+ + N$ jets (including no b quarks) to $W^+ + N$ jets (including two b quarks), and ratios of $Z^0/\gamma^* + N$ jets (including no b quarks) to $Z^0/\gamma^* + N$ jets (including two b quarks). Also given are the ratios $W^+ + b\bar{b} + N$ jets to $Z^0/\gamma^* + b\bar{b} + N$ jets .

the jargon that Z^0 means both amplitudes, as the source of the resulting final state that is measured by nature cannot be untangled.).

[25] G. Altarelli, R. Ellis, M. Greco, and G. Martinelli, Nucl. Phys. B **246** (1984).

[26] S. Geer and W. Stirling, Phys.Lett.B **152** (1985).

[27] R. Kleiss and W. J. Stirling, Nucl. Phys. B **262** (1985).

[28] M. L. Mangano and S. Parke, Phys. Rev. D **41** (1990).

[29] F. A. Berends, H. Kuijf, B. Tausk, and W. T. Giele, Nucl. Phys. B **357** (1991).

[30] F. A. Berends, W. T. Giele, H. Kuijf, R. Kleiss, and W. J. Stirling, Phys. Lett. B **224** (1989).

[31] R. K. Ellis, G. Martinelli, and R. Petronzio, Nucl. Phys. B **211** (1983).

[32] P. B. Arnold and M. H. Reno, Nucl. Phys. B **319** (1989), erratum-ibid. **330**, 284 (1990).

[33] P. Arnold, R. K. Ellis, and M. H. Reno, Phys. Rev. D **40** (1989).

[34] W. T. Giele, S. Keller, and E. Laenen, Phys. Lett. B **372** (1996).

[35] R. K. Ellis and S. Veseli, Phys. Rev. D **60** (1999).

[36] J. M. Campbell and R. K. Ellis, Phys. Rev. D **62** (2000).

[37] M. L. Mangano, M. Moretti, and R. Pittau, Nucl. Phys. B **632** (2002).

[38] M. L. Mangano, Nucl. Phys. B **405** (1993).

[39] T. Stelzer and W. Long, Comput. Phys. Commun. **81**, 357 (1994).

[40] F. Maltoni and T. Stelzer (2002), hep-ph/0208156.

[41] R. Ellis and S. Veseli, Phys. Rev D **60** (1999).

[42] J. M. Campbell and R. Ellis, Phys.Rev.D **62**, 114012 (2000).

[43] J. M. Campbell and R. Ellis, Phys.Rev.D **65**, 113007 (2002).

[44] M. Spiropulu, Ph.D. thesis, Harvard University (2000.), this is the first use of the ratios $\sigma(W+N\text{jets})/\sigma(Z^0/\gamma^* + N\text{jets})$ we have found; here they are used to normalize the W + N jets prediction to the Z + 2 jet data.

[45] The transverse momentum is defined as $p_T = p\sin\theta$; the transverse energy is defined as $E_T = E\sin\theta$. Missing transverse energy is defined as $\not\!\!E_T = -\Sigma E_T$, where the sum is over all objects in an event. We use the convention that 'momentum' refers to pc and 'mass' to mc^2, so that energy, momentum, and mass are all measured in GeV.

[46] D. Acosta et al. (CDF), Phys. Rev. D **65** (2002).

[47] By 'inclusive' we mean counting the number of jets $\geq N$ for each N; by 'exclusive' we mean counting exactly N jets.

[48] B. Abbott (D0) (1997), contributed to 18th International Symposium on Lepton and Photon Interactions (LP 97), Hamburg, Germany, 28 Jul - 1 Aug 1997.

[49] F. Abe et al. (CDF), Phys.Rev.D **45**, 1448 (1992).

[50] The proton and antiproton beams each consist of 36 bunches distributed around the 1-km radius Tevatron ring. Proton-antiproton interactions occur when the two beam cross each other; more than one collision can occur in a single crossing. The time-response of the detectors is typically such that the effects of multiple interactions are integrated over, with only partial discrimination between interactions being possible by reconstructing charged tracks to different vertex positions.

[51] The measurement and understanding of the jet E_T and η distributions is a major task for Run II and the LHC; the focus here is instead on the extent that the W and Z^0/γ^* cases cancel, and hence an estimate of the expected precision on the ratio.

[52] As the calorimeter response is calibrated by jet balancing in η the energy scales have a maximum excursion versus η of a few %. It is this uncertainty times the difference in the jet η distributions that sets the limit on the contributions to the ratio from the jet energy scale.

[53] T. Affolder et al. (CDF), Phys.Rev.D **65**, 092002 (2002).

[54] S. Kopp, Ph.D. thesis, University of Chicago (1994).

[55] F. Abe et al. (CDF), Phys. Rev. D **52** (1995).

[56] H. L. Lai et al., Eur. Phys. J. C **12**, 375 (2000), we use the interpolation rather than the table.

[57] A. Martin, R. Roberts, W. Stirling, and R. Thorne, Eur. Phys. J. **C4**, 463 (1998), hep-ph/9803445.

[58] A. Martin, W. Stirling, and R. Roberts, Int. J. Mod. Phys. **A10**, 2885 (1995).

[59] A more rigorous method, which would be appropriate at the time of an analysis of real data, is described in: W. T. Giele, and S. A. Keller, and D. Kosower, (2001), eprint hep-ph/0104052.

[60] Of course it is possible that a new source feeds both numerator and denominator in equal proportion; in that case this method has no sensitivity.

[61] With the larger dataset the uncertainties on such quantities as the u/d ratio, and hence the PDFs, the η and p_T distributions of W and Z production, and other quantities will also be better measured.